Synthesis and characterization of $CsSnI_3$ thin films

Kai Shum,[1,a)] Zhuo Chen,[1] Jawad Qureshi,[1] Chonglong Yu,[1] Jian J. Wang,[2] William Pfenninger,[2] Nemanja Vockic,[2] John Midgley,[2] and John T. Kenney[2]
[1]*Department of Physics, Brooklyn College of CUNY, Brooklyn, New York 11020, USA*
[2]*OmniPV Inc., 1030 Hamilton Ct., Menlo Park, California 94025, USA*

(Received 20 February 2010; accepted 11 May 2010; published online 2 June 2010)

We report on the synthesis and characterization of $CsSnI_3$ perovskite semiconductor thin films deposited on inexpensive substrates such as glass and ceramics. These films contained polycrystalline domains with typical size of 300 nm. It is confirmed experimentally that $CsSnI_3$ compound in its black phase is a direct band-gap semiconductor, consistent with the calculated band structure from the first principles. The band gap is determined to be ~1.3 eV at Γ point at room temperature. © *2010 American Institute of Physics*. [doi:10.1063/1.3442511]

An early study on the structural information of $CsSnI_3$ compound in form of powders was reported by Scaife *et al.*[1] in 1974. A few years later, a yellow, needlelike $CsSnI_3$ microcrystal was synthesized and its crystal structure was independently studied by Mauersberger and Huber.[2] No additional information was available until the discovery of another polymorph of this compound in 1991 by Yamada *et al.*[3] This polymorph was named as black $CsSnI_3$ since it had a lustrous black color. They found that the black polymorph of $CsSnI_3$ could be obtained through a phase transition from the yellow $CsSnI_3$ by increasing its temperature above 425 K. It was further demonstrated by differential thermal analysis and x-ray diffraction (XRD) that during the cooling of the black $CsSnI_3$ from 450 K, its ideal cubic perovskite structure (B-α) deformed to a tetragonal structure (B-β) at 426 K, and became an orthorhombic structure (B-γ) below 351 K. Experimental studies of electrical and optical properties of this compound have been hindered by lack of high quality $CsSnI_3$ samples either in bulk or thin film format. Only recently, aiming at the unique properties of hybrid organic-inorganic perovskites based on tin halides, Borriello *et al.*[4] calculated band structures of B-α, B-β, and B-γ from the first principles using the crystal structures published by Yamada *et al.*[3] It was concluded that all three structures had direct band gap (E_g) at Z, R, and Γ points for B-α, B-β, and B-γ, respectively, with $E_g(\text{B-}\alpha) < E_g(\text{B-}\beta) < E_g(\text{B-}\gamma)$.

Here we describe an effective and inexpensive method to synthesize high quality $CsSnI_3$ thin films on large-area substrates such as glass, ceramics, and silicon. These films are structurally characterized and contain polycrystalline domains with an average domain size of ~300 nm. Optical absorption and photoluminescence (PL) methods are used to demonstrate that this compound is indeed a direct band-gap semiconductor, consistent with the calculated from the first principles.[5] The value of its band gap is determined to be ~1.3 eV at room temperature.

The band structure of $CsSnI_3$ based on the energy-minimized structural coordinates is shown in Fig. 1. Three salient features of the electronic states near the band edges should be pointed out. First, it is clearly a direct band-gap semiconductor with a band gap at Γ symmetry point.[6] Second, the curvature of the lowest conduction band (CB1) is about two times smaller than the top valance band (VB1) indicating that the electron effective mass is larger than that of holes. Third, there is another conduction band (CB2) closely adjacent to CB1. They are parallel to each other in momentum space from Γ to S point. The electronic states of the CB1 is the *p*-orbital of the central tin atom of the SnI_6 octahedron; while the *p*- and *s*-orbital of the six outer iodine atoms of the octahedron equally contribute to the CB2 states. The electronic states of VB1 originate mainly from the *p*-orbital of iodine atoms.

The polycrystalline $CsSnI_3$ thin films were synthesized by a two-step method. In the first step, high purity multiple layers (usually six) of SnI_2 (or $SnCl_2$) and CsI were alternately deposited in vacuum (~10^{-5} Torr) on glass, ceramics, and silicon substrates by a combination of thermal and e-beam evaporators. A rapid thermal annealing was followed in a dry N_2 environment to activate a self-limiting chemical reaction[7] of CsI with SnI_2. In the case of $SnCl_2$, annealing can be done in air. Both CsI/SnI_2 and $CsI/SnCl_2$ layered thin film samples give an intense characteristic PL around 950 nm. The possible side products for the $CsI/SnCl_2$ layered samples are $CsSnCl_3$, $CsSnICl_2$, and $CsSnI_2Cl$. The first two have much larger band gaps than that of $CsSnI_3$, while the last one has a smaller band gap than that of $CsSnI_3$. Very weak PL relative to the 950 nm emission were observed for a $CsI/SnCl_2$ layered sample and their PL peak positions are consistent with the calculated band gaps for $CsSnCl_3$ and $CsSnICl_2$. No PL or absorption features around 1.5 μm were

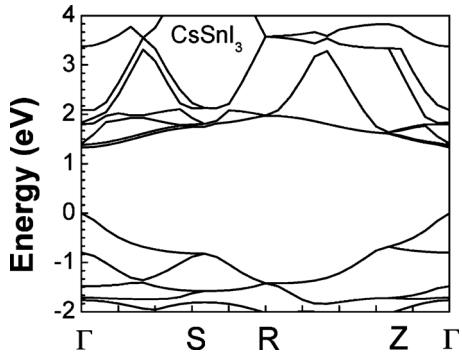

FIG. 1. Calculated electronic band structure of $CsSnI_3$. The theoretically calculated band-gap value from the first principle is known to be underestimated; the experimentally measured band-gap value of ~1.3 eV at 300 K is used.

a)Electronic mail: kshum@brooklyn.cuny.edu.

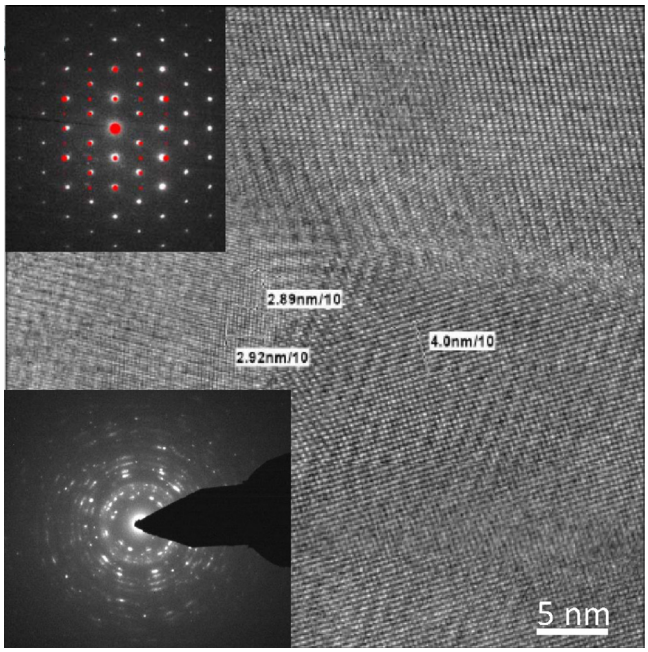

FIG. 2. (Color online) High resolution TEM measured in a triple-domain area. Bottom-left inset: electron diffraction pattern in a selected area where many domains are orientated in different directions. Top-left inset: an electron diffraction pattern in a selected area where a single large domain exists, along with a calculated pattern (solid dots) superimposed on the measured pattern.

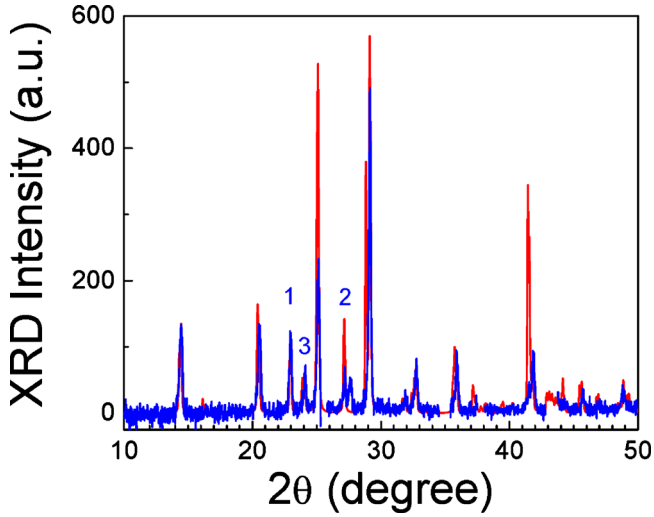

FIG. 3. (Color online) Measured XRD intensity as 2θ is compared with the calculated curve, matching main features of the γ-crystal structure of $CsSnI_3$ as indicated by "1, 2, and 3." The XRD peaks from the ceramic substrate are removed for clarity.

observed corresponding to the $CsSnI_2Cl$ band gap. Hence these possible side products from $CsI/SnCl_2$ layered samples do not affect the intense band edge emission of $CsSnI_3$ reported here.

$CsSnI_3$ thin films were characterized by the surface and cross-section scanning electron microscopy and transmission electron microscopy (TEM). The films are polycrystalline with a typical domain size of ~300 nm. TEM images were taken from several selected areas, showing different lattice spacing due to different crystal orientations. Figure 2 shows the TEM image of a $CsSnI_3$ film on a glass substrate in a triple-domain area. Electron diffraction patterns were also measured. Our polycrystalline films gave typical ringlike patterns, as shown by the bottom-left inset in Fig. 2. In large domain areas, electron diffraction patterns can present single crystal features. We compare the measured and calculated electron diffraction patterns (superimposed red dots) as displayed in the top-left inset of Fig. 2. 20 sets of crystal planes in the [201] direction of theoretical crystal structure $CsSnI_3$ are matched.[8,9]

The crystal structure of polycrystalline films is further verified by XRD data shown in Fig. 3 as the blue curve using a CsI/SnI_2 layered sample with a one-to-one stoichiometric ratio on a ceramic substrate. The numbers of "1" and "2" indicate the expected XRD features of the Sn–I–Sn bond tilting in the *a*- and *b*-directions, respectively, while "3" represents the signature of the Sn–I–Sn bond tilting in the *c*-direction. These features match the calculated XRD intensity (red curve) for $CsSnI_3$.[8]

PL spectra were extensively used to characterize the synthesized films under various conditions. They were taken from a Nanolog system from Horiba Jobin Yvon. It consists of a light source (450 W Xe-lamp), a double-grating excitation spectrometer to select a central excitation wavelength and its bandwidth, a sample compartment either fiber-coupled or in free-space to collect PL, and an emission spectrometer to spectrally select desired emission to a photomultiplier tube (Hamamatsu P2658P) coupled with single photon counting electronic circuits. Photoexcitation level is low and is about 20 mW/cm^2. Absorption spectra of $CsSnI_3$ thin films were measured by a Lambda-950 ultraviolet-visible-infrared (UV-VIS-IR) spectrometer equipped with a 60 mm integrating sphere from Perkin Elmer.

The annealing temperature (T_a) and time duration (Δt_a) dependences of the characteristic PL from $CsSnI_3$ thin films were studied. The peak position of PL does not depend on either annealing temperature or time duration used for the annealing. However, the intensity of PL is strongly dictated by annealing conditions. The optimal condition for the strongest PL intensity depends on a given sample. For a thin film with $CsI/SnCl_2$ layers on a glass substrate, a typical annealing temperature of ~190 °C with time duration of ~15 s will result in a good polycrystalline film, having very intense PL at ~950 nm. For a film with CsI/SnI_2 layers, annealing temperature is higher than 190 °C since the melting temperature of SnI_2 (320 °C) is higher than that of $SnCl_2$ (247 °C). Figure 4 displays the PL spectra taken from the selected pieces of CsI/SnI_2 layered samples cut from a same Si substrate annealed at different temperatures for 20 s. The integrated area of PL spectrum at each annealing temperature is summarized in the inset of this figure. It shows two regions: below and above 330 °C which is close to the melting temperature of SnI_2. Several observations can be made although the thermal dynamics for the chemical reaction to form $CsSnI_3$ is not understood. The characteristic PL starts as low as 200 °C and reaches to a local maximum at 260 °C before weakening to near zero level. Right after 330 °C, it immediately extends to the second maximum around 370 °C, which is four times larger than the PL intensity at 260 °C. It should be also mentioned that $CsSnI_3$ films will degrade in a few days under a normal ambient condition without any protections. However, if they are stored in dry N_2 gas or encapsulated, they can be free of degradation.

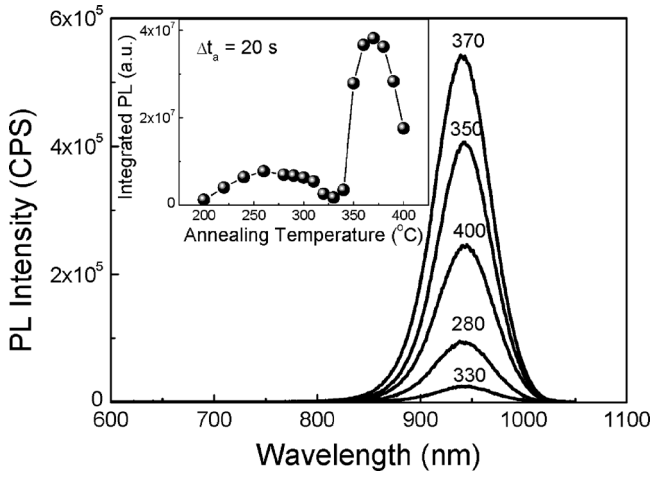

FIG. 4. PL spectra of CsI/SnI_2 layered samples on a same silicon substrate taken at different thermal annealing temperatures of 370, 350, 400, 280, and 330 °C from top to bottom. The inset displays the integrated PL spectrum at different annealing temperatures.

Optical absorption spectra of $CsSnI_3$ thin films were measured at room temperature. A typical absorption spectrum of $CsI/SnCl_2$ layered films deposited on ceramics is displayed in Fig. 5 along with the PL spectrum taken from the same film. The absorption contribution from the substrate was removed and scatterings were considered through the integrating sphere. The absorption spectrum reflects the nature of the inhomogeneity of the film in terms of composition and domain sizes. The value of the absorption coefficient steeply takes off after the PL emission peak and is zero below it. This behavior is a testimony for the direct band gap of $CsSnI_3$.[10] The shoulder riding on the absorption curve, ~50 meV away from the PL peak position, may associate with the second conduction band CB2 although more work is needed to fully understand the nature of absorption in $CsSnI_3$ thin films. It should be emphasized that the PL is very intense under a weak photoexcitation indicating very high quantum efficiency, which is supportive to our direct band-gap assertion for the $CsSnI_3$ compound as predicted by calculations from the first principles. The PL line shape is inhomogeneously broadened with a spectral width of ~50 meV.

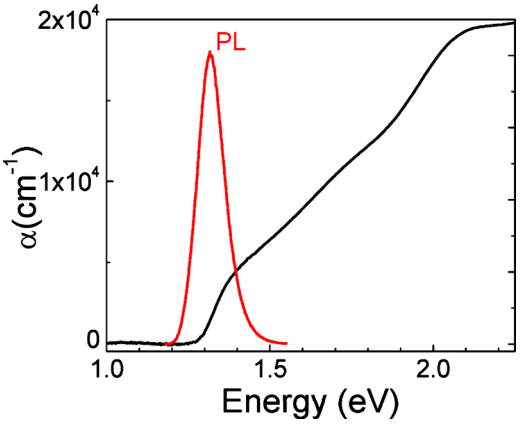

FIG. 5. (Color online) Measured absorption and PL spectra at room temperature for a $CsI/SnCl_2$ layered sample on a ceramic substrate.

In summary, we have described a long overlooked perovskite semiconductor compound $CsSnI_3$. The synthesis of its high optical quality polycrystalline thin films is demonstrated. Using the quantum mechanical simulation tools and the methods of PL and optical absorption, we have verified that it is a direct band-gap semiconductor with a band gap of ~1.3 eV at 300 K. This work optically authenticates another member of the semiconductor family and opens the door to explore its optical and electrical properties.

This work at Brooklyn College was partially supported by OmniPV Corporation and the Photonics Program of the City University of New York. We appreciate useful discussions with Mark Kobrak.

[1] D. Scaife, P. Weller, and W. Fisher, J. Solid State Chem. **9**, 308 (1974).
[2] P. Mauersberger and F. Huber, Acta Crystallogr., Sect. B: Struct. Crystallogr. Cryst. Chem. **B36**, 683 (1980).
[3] K. Yamada, S. Funabiki, H. Horimoto, T. Matsui, T. Okuda, and S. Ichiba, Chem. Lett. **20**, 801 (1991).
[4] I. Borriello, G. Gantel, and D. Ninno, Phys. Rev. B **77**, 235214 (2008).
[5] CASTEP simulation tool was used for this work; www.accelrys.com. The computational results on the total potential energy and electronic states of a given crystal structure were based on the density functional module CASTEP. Prior to the energy band structure calculation of a crystal structure, the type of crystal structure was determined by an energy minimization procedure in which the potential energy was calculated by varying a lattice scaling factor, by fine-tuning the Sn–I–Sn (or Sn–Cl–Sn) titling angles in *ab*-plane and in *c*-direction, as well as by changing Cs positions.
[6] Other symmetry points shown in Fig. 1 are as follows: S ($-0.5a_k$, $0.5b_k$, and 0), Z (0, 0, and $0.5c_k$), and R ($-0.5a_k$, $0.5b_k$, and $0.5c_k$), where $a_k = \pi/a$, $b_k = \pi/b$, and $c_k = \pi/c$.
[7] We have experimented different stoichiometric ratios of CsI to SnI_2 (or $SnCl_2$). The resulting films always give a characteristic PL emission peak around 950 nm although its intensity varies slightly. We have also characterized various samples using x-ray fluorescence (XRF) and energy dispersive x-ray analysis (EDS). For an example, with the 1-to-1 ratio of CsI/SnI_2, an atom ratio was found by XRF to be 1:0.9:2.3 for Cs:Sn:I after annealing, indicating slight loss of tin and iodine atoms during annealing. The EDS spectra were also acquired at various locations of annealed samples with no separated regions of CsI and SnI_2 (or $SnCl_2$ in case of $CsI/SnCl_2$ layered samples). For the fixed 1-to-1 stoichiometric ratio, the chemical formula for the CsI/SnI_2 reaction is $CsI+SnI_2 \rightarrow CsSnI_3$; while for the $CsI/SnCl_2$ reaction, three possible reactions that lead to $CsSnI_{3-x}Cl_x$ (x=0, 1, 2, and 3) structures are as follows: (1) $CsI+SnCl_2 \rightarrow CsSnICl_2$, (2) $2CsI+2SnCl_2 \rightarrow CsSnI_2Cl+CsSnCl_3$, and (3) $3CsI+3SnCl_2 \rightarrow CsSnI_3+2CsSnCl_3$.
[8] CRYSTALMAKER simulation package (www.crystalmaker.com) was used to generate the electron diffraction patterns and XRD traces using the $CsSnI_3$ unit cell obtained through our energy-minimization procedure.
[9] The matching planes in sequence of diffraction efficiency from 47% to 3% are as follows: $(\bar{2}24)$, $(\bar{2}\bar{2}4)$, $(2,\bar{2}4)$, $(22\bar{4})$, $(0\bar{4}0)$, (0 4 0), $(0\bar{2}0)$, (0 2 0), $(\bar{1}\bar{3}2)$, $(1\bar{3}\bar{2})$, $(\bar{1}32)$, $(13\bar{2})$, $(\bar{1}\bar{1}2)$, $(1\bar{1}\bar{2})$, $(\bar{1}12)$, $(11\bar{2})$, $(\bar{2}04)$, (204), $(\bar{2}44)$, and $(\bar{2}\bar{4}4)$.
[10] *Optical Processes in Semiconductors*, edited by J. I. Pankove (Dover, New York, 1971).